Fragmentation of condensed-phase DNA components by hyperthermal He^+ impact

Zongwu Deng, Marjorie Imhoff, Ilko Bald,* Eugen Illenberger,* and Michael A. Huels†
Department of Nuclear Medicine and Radiobiology, Ion Reaction Laboratory, Faculty of Medicine and Health Sciences, University of Sherbrooke, Sherbrooke, Quebec, Canada J1H 5N4
(Received 22 April 2006; published 24 July 2006)

We have observed severe damage to films of DNA components (thymine, D-ribose, 2-deoxy-D-ribose, and thymidine) induced by 10 to 100 eV He^+ ions (2.5–25 eV/amu). The damage is attributed to the kinetic and potential energies, as well as the chemical reactivity of the He^+ projectiles. Hyperthermal He^+ ion impact on these films results in the complete destruction of the molecules via fragmentation, and direct and indirect (secondary fragment) reactive scattering, all of which leads to the desorption of abundant cation and anion fragments. The chemical composition of the fragments is identified, and the fragmentation patterns are compared to those produced by Ar^+ irradiation. While the lower mass of He^+ ions causes less efficient desorption of very heavy fragments, several reactive collisions are also observed, including hydrogen abstraction by incident He^+ from any of the molecules studied to yield desorbing HeH^+. This process likely occurs via the formation of an intermediate molecular ion $(He\text{-}H\text{-}R)^{*+}$, which decays to $HeH^+ + R^{\bullet}$. Compared to Ar^+, here a significant ($\times 23$) enhancement in H^+ desorption is observed during He^+ ion irradiation, which likely involves (a) the decay of the intermediate $(He\text{-}H\text{-}R)^{*+}$, or desorbing HeH^+, and (b) Auger or quasiresonant excitations of C, N, or O atom centers (or C-H, N-H, or O-H bonds) by the incident He^+ ion. The formation of several molecular cations, e.g., H_3O^+, also requires hydrogen abstraction from its parent or adjacent molecules by initial cation fragments prior to desorption.

DOI: 10.1103/PhysRevA.74.012716 PACS number(s): 34.50.Dy, 82.30.Fi, 87.14.Gg

I. INTRODUCTION

Ionizing radiation is a common modality of cancer therapy, including the conventional use of high energy electron and photons (x rays and γ rays), and more recently, high energy protons or heavy ions (from He up to Ar); the latter is under rapid development with significant clinical success [1,2]. Ionizing radiation treatment of biological media causes severe damage to DNA, mainly due to the production of single and double strand breaks of DNA, and clustered genotoxic lesions [3]. DNA damage is due not only to the primary radiation itself but also to the abundant secondary particles produced along the radiation track [4], both of which strongly depend on the radiation modality. The secondary particles include low-energy ions, radicals, excited neutrals, and ballistic secondary electrons [5,6]. Reactions of these early transients with the surrounding medium lead to substantial physical and chemical modifications, and determine the starting input for all the further, diffusion-limited, radiation chemistry and its eventual biological end points.

However, compared to the extensively studied electron (both solvated and unsolvated) and radical reactions leading to DNA damage [3,7–9], our understanding of the nascent primary or secondary ion interactions with DNA at the nanoscopic molecular level is still rudimentary, particularly in the low energy, viz., sub keV range corresponding to either primary ion track ends, or secondary ion energies. Secondary ion interactions with biomolecules may be initiated by all types of ionizing radiations which produce secondary ions in different charge states (positive or negative, single or multiple charge), and with very different potential and kinetic energies as well as chemical reactivities. In heavy ion therapy, when a primary ion penetrates a biomedium, a large amount of secondary ions (fragments) are produced with thermal energies up to several hundreds of eV and different charge states [10,11]. Conventional radiation (electrons and photons) can also produce secondary ions, but only with energies from thermal up to tens of eV, depending on their formation dynamics, such as decay of valence or core excitations [12–14]. Any of these secondary ions are capable of causing physical and chemical damage to DNA molecules in subsequent scattering events. It has been demonstrated that Ar^+ ions with energy down to 10 eV can effectively fragment DNA components, leading to the formation of abundant nonthermal cation and anion fragments, and induce physicochemical reactions such as hydrogen abstraction by the initial fragments [15–18]. More reactive ions such as N^+ and N_2^+ can cause further damage via specific physicochemical reactions at even lower energies [19]. Recently, there has been a study on the interaction of keV He^+ with gas phase sugar molecules where extensive statistical fragmentation of the molecules was observed [20].

Here we investigate the interaction of 10–100 eV He^+ ions with films containing several fundamental DNA components, including a nucleobase (thymine), the sugar molecules D-ribose and 2-deoxy-D-ribose, and a nucleoside (thymidine). Our interest in He^+ ions is motivated by several aspects: (1) it has much less mass than most of the other ions of interest (e.g., C^+ or Ar^+) so that we can obtain insight into the effects of ion mass on fragmentation efficiency of biologically relevant molecules at such low energies; (2) its first

*Permanent address: Institut für Chemie, Physikalische und Theoretische Chemie, Freie Universität Berlin, Takustrasse 3, D-14195 Berlin, Germany.
†Corresponding author. FAX: (819) 564-5442; Email address: michael.huels@USherbrooke.ca

 ©2006 The American Physical Society

ionization potential (24.6 eV) is much higher than many other ions [e.g., 15.7 eV for Ar^+, which however, still falls into the range of valence ionization (excitation)], and may play a role in molecular excitation (dissociation) leading to damage. For example, it was observed that He^+ ions or metastable He atoms, both with a 1 s hole, can induce H^+ desorption from OH-adsorbed surfaces via quasiresonant or Auger processes [21–23]; (3) the He^+ ion is chemically reactive and can form a stable ionic molecule HeH^+ during impact with H_2 or hydrogen-containing molecules [24–27]; (4) while energetic α particles (viz., He^{2+}) from internal (e.g., radon) or external (space radiation) sources are known to efficiently damage cellular DNA, the initial spectrum of damage induced in DNA at the molecular level is as of yet unknown, particularly at or near the α-particles track ends, when their velocities are greatly lowered, and thus their charge state is reduced to +1 (He^+). The present work is a first attempt to investigate some of these effects on ion-molecule interactions in general, and their implications for our basic understanding of ion induced damage at the nanoscopic level to the fundamental components of DNA.

II. EXPERIMENTAL METHOD

The experiments were conducted in Sherbrooke on a hyperthermal ion beam apparatus, developed in-house, which delivers a highly focused mass- and energy-resolved positive or negative ion beam in the 1–500 eV energy range into an ultrahigh vacuum reaction chamber for sample irradiation. The system and experimental procedure will be described in great detail elsewhere. Briefly, He^+ ions are produced in an electron impact gas discharge ion source, extracted and focused by a series of lenses into a custom-designed magnetic mass analyzer for mass selection. The mass-selected ions are then refocused, decelerated, and finally directed to the target. Ion energies are defined by the electrical potential difference between the ion source and the target, and measured by retardation methods. He^+ ion currents of 120–180 nA are used for the present experiments, with an energy spread of ~1 eV full width at half maximum over the entire energy range. The base pressure in the vacuum system is $\sim 10^{-9}$ Torr. The pressure in the ion source chamber during experiments increases to nearly 10^{-5} Torr, while the pressure in the target chamber remains at 10^{-9} Torr with the assistance of four differential pumping stages.

A high-resolution quadrupole mass spectrometer (QMS) (IDP 300 triple filter, mass range 0.4–200 amu, Hiden Analytical Ltd.) is installed perpendicularly to the axis of the ion beam to monitor desorbing ionic products during ion-beam impact on molecular films. The mass spectrometer is designed to measure ions with *in vacuo* energies between 0 and 5 eV. It was modified by the manufacturer from a standard ion desorption probe (IDP 300, with mass range from 0.4–300 amu) to yield better sensitivity and mass resolution at lower masses such as H and D. A large diameter lens is used at the entrance of the QMS to ensure a large solid angle of acceptance, and thus a higher sensitivity for the desorbing ions. The sample holder is located in the center of the reaction chamber. During experiments the sample is placed ~2 cm away from both the exit of the ion beam and the entrance of the QMS, with its surface oriented at 30° with respect to the incident ion beam axis, and at 60° relative to the QMS central axis.

Films of biomolecules of variable thickness are prepared by *in vacuo* evaporation onto an atomically clean polycrystalline Pt substrate held at room temperature. In the present experiments, a particular substance (all are at least 99% pure, purchased from Aldrich and used without further purification) is loaded in a miniature oven contained in a load-lock chamber, and degassed by gentle heating for several hours well below its evaporation onset. The evaporation-deposition rate is monitored *in situ* and calibrated in the load-lock chamber by a quartz crystal microbalance, and characterized in $ng/cm^2/min$. The film mass (thickness) is then determined by the known deposition rate and time. The Pt substrate is cleaned by flash heating up to 1000 °C prior to each film deposition, and its cleanliness is verified by 200 eV Ar^+ SIMS. Ion stimulated desorption (ISD) of ions from thymine and thymidine films exhibits a strong dependence on the film thickness [17]. It is found that films of 100–400 ng/cm^2 provide a good thickness range for measuring the ionic fragment desorption. The D-ribose and 2-deoxy-D-ribose films undergo a certain evaporation loss at room temperature under ultrahigh vacuum conditions due to their high volatility [18]. As a consequence, the results in this work were obtained from films of 200 ng/cm^2 thymine and thymidine, 800 ng/cm^2 D-ribose and 2000 ng/cm^2 2-deoxy-D-ribose, respectively. Based on the density of the molecules, the above thicknesses correspond roughly to 4 *nominal* monolayers (ML) of thymine and thymidine, and 20 and 50 nominal ML of D-ribose and 2-deoxy-D-ribose, respectively, assuming even coverage as discussed elsewhere [15–18].

III. RESULTS AND DISCUSSION

Figure 1 shows typical mass spectra of both cation and anion fragments produced by 100 eV He^+ ion irradiation of films of (a) 200 ng/cm^2 thymine (T), (b) 800 ng/cm^2 D-ribose (*R*), (c) 2000 ng/cm^2 2-deoxy-D-ribose (*dR*) and (d) 200 ng/cm^2 thymidine (*dT*). Most of the fragments are identified and marked in the mass spectra. The chemical identification of the fragments of thymine is achieved by comparing the present mass spectra of condensed phase thymine, and thymine-methyl-d_3-6-*d* (not shown), produced here by He^+, to previous data on Ar^+ ion irradiation in the condensed phase, and electron impact (70 eV) in gas phase [16]. For He^+ impact the major cation fragments from thymine are H^+, CH_2^+, CH_3^+, $C_2H_3^+$, $HNCH^+$, $C_3H_3^+$, with trace amounts of $OCNH_2^+$, $HNC_3H_4^+$ (±H), $[T\text{-OCN}]^+$, $[T\text{-OCNH}_2]^+$, $[T\text{-O}]^+$, $[T+\text{H}]^+$, etc. The major anion fragments are H^- and O^-. Notably, the most abundant cation fragment at 28 amu is assigned uniquely to a $HNCH^+$ ion, originating exclusively from bond cleavage at the N1-C6 site of thymine, rather than a possible CO^+ ion [16]. In the anion mass spectrum of (a), two significant anion fragments CN^- and OCN^- that desorb during Ar^+ ion irradiation [15–17] are negligible here during He^+ ion irradiation.

The identification of the fragments of D-ribose (b) and

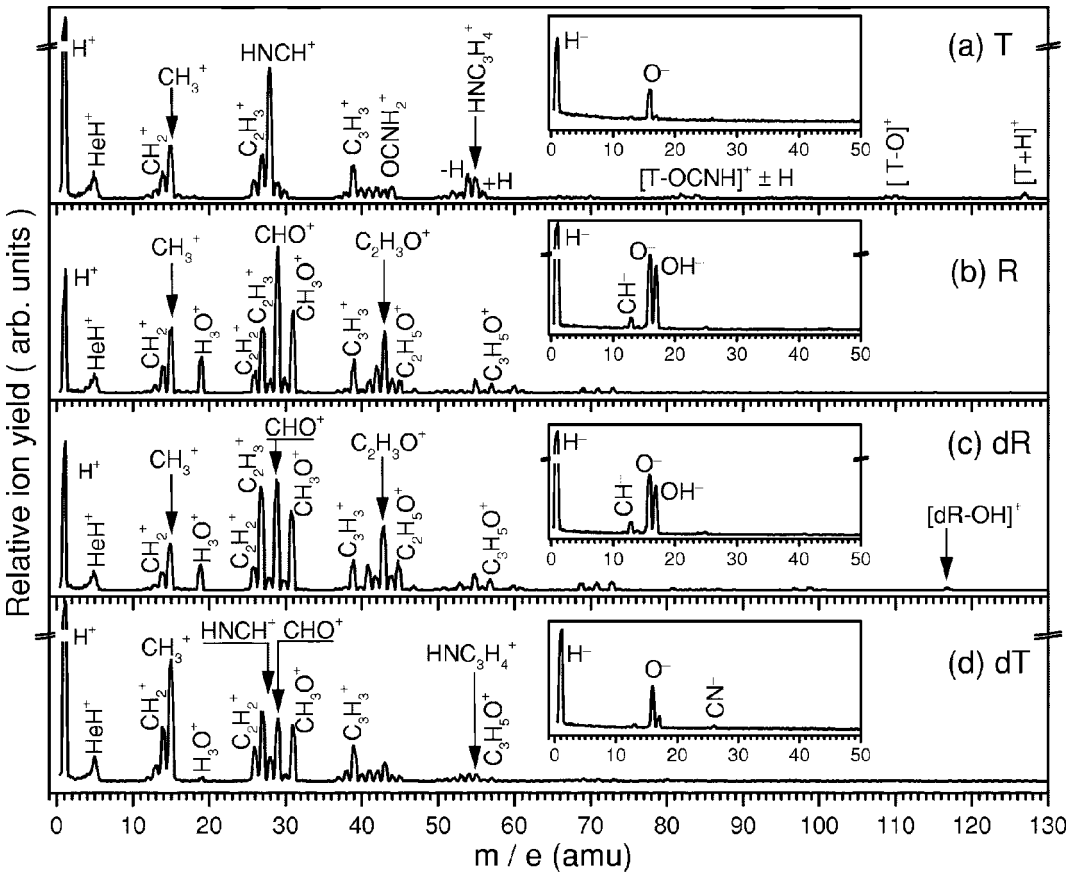

FIG. 1. Typical cation and anion (insets) fragment patterns of ion stimulated desorption from films of (a) 200 ng/cm^2 thymine (*T*), (b) 800 ng/cm^2 D-ribose (*R*), (c) 2000 ng/cm^2 2-deoxy-D-ribose (*dR*), and (d) 200 ng/cm^2 thymidine (*dT*), on a Pt substrate produced by 100 eV He^+ ion irradiation. Note that there are breaks in the ordinates of some of the mass spectra in order to show the lower yield fragments.

2-deoxy-D-ribose (c) is achieved by measuring and comparing the present mass spectra of D-ribose, isotope-labeled D-ribose (5-^{13}C and 1D D-ribose, from Cambridge isotopes, 98% isotopic purity, not shown), and 2-deoxy-D-ribose, to previous data on Ar^+ impact [18]. For He^+ irradiated films these fragments include cations H^+, CH_2^+, CH_3^+, H_3O^+, $C_2H_2^+$, $C_2H_3^+$, CHO^+, CH_3O^+, $C_3H_3^+$, $C_2H_3O^+$, as well as anions H^-, CH^-, O^-, OH^-, etc. The low intensity at 28 amu of the cation mass spectra also suggests the absence of a CO^+ ion. The identification of He^+ induced thymidine fragments (d) is therefore accomplished here by comparison with those of thymine (a) and 2-deoxy-D-ribose (c) (thymidine is a nucleoside formed via a glycosidic bond between N1 of thymine and C1 of 2-deoxy-D-ribose)[15]. It appears that for He^+ impact most of the fragments originate from its sugar moiety, similar to Ar^+ irradiation [15].

On first sight the fragment patterns of the four molecules studied here by He^+ ISD are similar to those obtained during Ar^+ ion irradiation.[15–18] However, several significant differences can also be observed. Figure 2 shows mass spectra of ionic fragments of 2-deoxy-D-ribose produced by 100 eV (a) Ar^+ and (b) He^+ ion irradiation for comparison. During He^+ ion irradiation a significant increase (decrease) in relative intensity of light (heavy) fragments is observed in the cation fragment spectra, particularly the H^+ fragment. The relative intensities of CH_2^+ to CH_3^+ and $C_2H_2^+$ to $C_2H_3^+$ also increase in the case of He^+ ion irradiation. Such differences are also observed for the other three molecules. In addition, a cation product at 5 amu is also observed in all cases of He^+ irradiation, and is assigned to HeH^+. As for the anion frag-

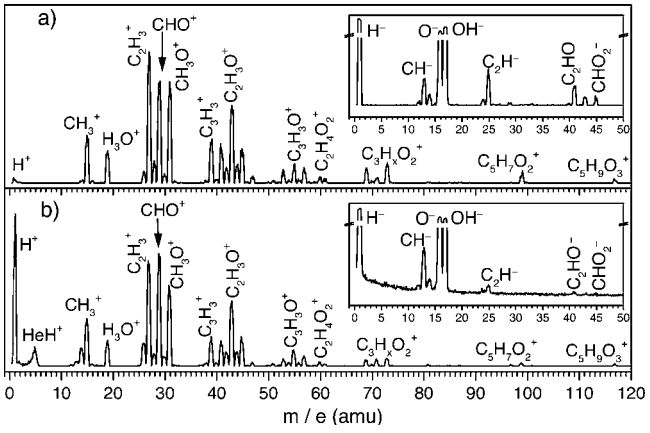

FIG. 2. Typical cation and anion (insets) fragment patterns of ion stimulated desorption of 2000 ng/cm^2 2-deoxy-D-ribose films on a Pt substrate produced by 100 eV (a) Ar^+ and (b) He^+ ion irradiation. Note that there are breaks in the ordinates of the anion mass spectra in order to show the lower yield fragments.

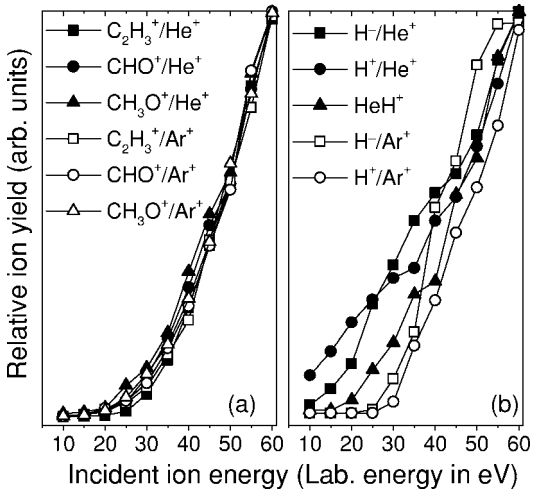

FIG. 3. Desorption energy thresholds of (a) major cation fragments and (b) H^-, H^+, and HeH^+ fragments produced by He^+ and Ar^+ ion irradiation of 800 ng/cm^2 D-ribose films on a Pt substrate. All ion yields are normalized here in intensity at 60 eV for ease of comparison. Similar desorption energy thresholds are found for fragments of 2-deoxy-D-ribose films (not shown).

ments, the major difference to Ar^+ ISD is that the CN^- and OCN^- ring fragment anions (from the base) are negligible during He^+ ion irradiation of thymine and thymidine films.

Figure 3 shows the relative desorption yields of (a) major cation fragments and (b) H^-, H^+, and HeH^+ fragments produced by He^+ and Ar^+ ion irradiation of D-ribose films as a function of incident ion energy, from which the fragment desorption energy thresholds are derived. While the major fragments appear at similar energies (down to 15–20 eV) in both cases, H^- and H^+ fragments appear at lower energies during He^+ ion irradiation than Ar^+ ion irradiation, particularly the H^+ fragment which appears with high intensity even at 10 eV or lower. Similar energy thresholds of fragment desorption are also obtained in the cases of the other three molecules (not shown).

The desorption dynamics under present film conditions have been discussed in detail elsewhere for the case of Ar^+ ion irradiation of thymine and ribose films, and is concluded to be kinetic [17,18]. It is believed that the same dynamics also govern the formation of most of the fragments observed here during He^+ ion irradiation but are modulated by the difference in mass and potential energies of the He^+ projectiles. Here we give a brief discussion and later focus on the formation of H^+ fragments and HeH^+ ions. The cation fragment desorption involves both kinetic and potential energy transfer from the incident ions. A target molecule is positively ionized and thus excited via charge exchange with the incident ions. Subsequent momentum transfer breaks the molecule into fragments and provides the required kinetic energy for the ionic fragments to overcome the image charge induced polarization potential to desorb from the film [17].

Using a classical binary collision approximation, the maximum kinetic energy (in the laboratory frame) that can be transmitted to a target particle (molecule or atom center) by momentum transfer from the low energy incident ion is $4m_1m_2/(m_1+m_2)^2E_{lab}$, where m_1 and E_{lab} are the mass and the laboratory kinetic energy of the incident particle, respectively, and m_2 is the mass of the specific target involved in the collision. Qualitatively, more kinetic energy can be transferred to the target when its mass is closer to that of the projectile. This suggests a much lower efficiency of kinetic energy transfer to the heavy fragments from the He^+ ion than from the Ar^+ ion. Hence, the decrease in relative intensity of the very heavy fragments observed here can be partly ascribed to the less efficient momentum transfer from the lighter incident He^+ ion to the target molecule.

As noted previously [18], the formation of several cation fragments such as CH_3^+ and $C_2H_3^+$ from sugars, and H_3O^+ in general requires hydrogen abstraction by the original fragments such as CH^+/CH_2^+, $C_2H_2^+$, OH^+/H_2O^+, respectively, from its parent or an adjacent molecule. The increase in the relative intensity of CH_2^+ to CH_3^+ and $C_2H_2^+$ to $C_2H_3^+$ during He^+ ion irradiation compared to Ar^+ (Fig. 2) is also likely due to the less efficient momentum transfer by the latter to the original fragments, which is required for the subsequent hydrogen abstraction. However, the formation of the H_3O^+ ion appears to be largely independent of projectile for sugars (Fig. 2), i.e., the momentum transfer efficiency, but is largely reduced with respect to the other cation fragments in the case of thymine and thymidine. While this is not completely understood, it is likely that in sugars H_3O^+ is produced more efficiently via direct water (or H_2O^+) elimination at -OH sites and subsequent proton (or H) abstraction prior to desorption; this is in part supported by the observation of the H_2DO^+ formation involving the -Cl(D)-OH site in 1D D-ribose during either Ar^+ or He^+ impact, and the general absence of OH^+ desorption.

It is believed that the anion fragments (H^-, O^-, and OH^-) are formed via close collisions between incident ions and targeted atoms of relevance. It is likely to occur in cases where the positive charge of the incident ion is not successfully transferred to the target atom center in a molecule but rather induces a severe negative polarization on it along the chemical bond(s) linking it to the rest of the molecule. Subsequent momentum transfer causes chemical bond breaking along this bond(s), and ultimately produces an anion product. This is consistent within the framework of the bond breaking model [28,29]. H^- desorption induced by both He^+ and Ar^+ irradiation is believed to follow this dynamics, and its lower desorption energy threshold during He^+ ion irradiation can be partly accounted for by the more efficient momentum transfer due to the better match between the masses of H and He (quasisymmetric scattering), compared to H and Ar. In addition, their match in atomic size and orbital symmetry may induce bond polarization more efficiently, and thus facilitate the subsequent bond breaking. It is also possible that in thin films (e.g., submonolayer thymine films) a neutral hydrogen fragment picks up an electron from the film or the substrate to desorb as an anion [17].

Both O^- and OH^- are likely a result of a collision between an incident ion and an oxygen atom center of the molecules. However, OH^- is negligible during He^+ ion irradiation of thymine films due to the absence of a hydroxyl group. For thymine a channel to form OH^- via hydrogen abstraction by O or O^- fragments is nearly closed, likely because less momentum is transferred from the lighter He^+ projectile to the

C═O groups to yield sufficiently energetic O or O^- that can abstract a hydrogen and desorb. For the sugars, on the other hand both He^+ and Ar^+ can yield OH^- directly from the hydroxyl groups likely via strong polarization along the C-OH sugar bond. A significant difference between He^+ and Ar^+ ion irradiation (see Refs. [15–17]) is the much less efficient desorption of CN^- and OCN^- anions from thymine and thymidine films during He^+ impact. This cannot be ascribed merely to the less momentum transfer to the fragments in terms of the required kinetic energy for desorption of such heavy fragments, given the desorption of abundant multiple heavy-atom cation fragments (e.g., $C_2H_3^+$, CHO^+, $C_2H_3O^+$, etc.) during He^+ impact. Hence, we believe that the less efficient momentum transfer by He^+ to the endocyclic OCN and CN moieties in thymine or thymidine may also lead to less favorable orientations (i.e., distortion) of the chemical bonds in the ring that need to be dissociated for the formation and desorption of CN or OCN fragments, and/or a reduced efficiency of charge pickup from the substrate or film by the resultant CN and OCN fragments, if any are formed.

In this respect, the significant increase in H^+ desorption during He^+ ion irradiation cannot be accounted for exclusively by better momentum transfer, given the significant H^- desorption during Ar^+ ion irradiation (see the insets in Fig. 2). This is also implied by the *significantly* lower desorption energy threshold of H^+ during He^+ impact compared to Ar^+ ion irradiation. In order to obtain insight into the H^+ desorption dynamics, its formation site has to be determined. Its origin from isolated hydrogen adsorbed on a Pt substrate is ruled out given the film thickness of D-ribose and 2-deoxy-D-ribose studied here. Hence, H^+ desorption results from interactions between incident He^+ ions and the individual molecules. Its chemical origin can be further resolved by using isotope-labeled molecules since C-H, N-H, and O-H bonds are all involved in the molecules studied here.

The contribution to H^+ formation from C-H and N-H bonds in thymine is determined by using thymine-methyl-d_3-6-*d*. Figure 4 shows the cation mass spectra between $m/e=0.4$ and 8 for (a) thymine and (b) thymine-methyl-d_3-6-*d* obtained at several different He^+ energies. Both D^+ and H^+ ions are observed from thymine-methyl-d_3-6-*d* films, suggesting H^+ (D^+) formation from both N- and C-bound hydrogen of thymine. The branching ratio of D^+/H^+ in this energy range is deconvoluted and calculated to be about 3.0, suggesting a slight preference for C-bound deuterium (in contrast to the stoichiometric D/H ratio of $2\div1$ in thymine-methyl-d_3-6-*d*).

D^+ is also observed during He^+ ion irradiation of 1D D-ribose (not shown), suggesting contributions of C1-H sites to H^+ desorption from D-ribose. The calculation of its relative intensity to H^+ indicates that about 48% of H^+ originates from C-H and about 52% from O-H sites in sugars. Hence, He^+ induced H^+ desorption is more or less independent of the nature of the chemical bonds.

Many different dynamics have been proposed to account for electron, photon, or ion stimulated H^+ desorption from surfaces. In a study of ultraviolet photon stimulated H^+ desorption from dissociatively adsorbed water on Ti surfaces the photon energy threshold of H^+ desorption was found to be ~25 eV, close to the O 2*s* energy level, with a second

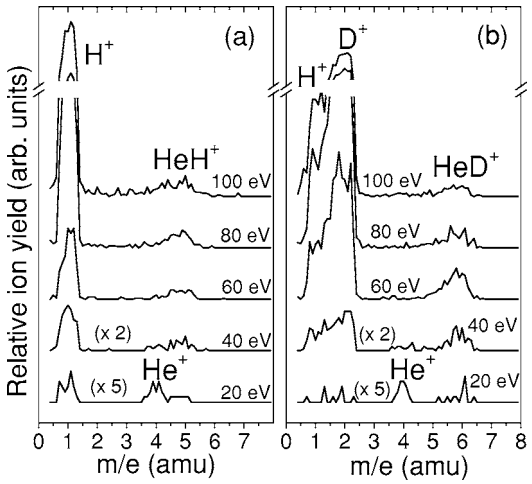

FIG. 4. Single scan cation mass spectra between 0.4–8 amu of (a) thymine and (b) thymine-methyl-d_3-6-*d* at several different incident He^+ ion energies. Note the appearance of a peak at 5 amu of thymine and a peak at 6 amu of thymine-methyl-d_3-6-*d*, suggesting the formation of HeH^+ and HeD^+ ions, respectively.

threshold close to the Ti 3*p* level. This suggested the involvement of O 2*s* and Ti 3*p* core hole excitations in the H^+ desorption dynamics [30]. Multicharged ion bombardment of hydrogen-contaminated surfaces also leads to abundant secondary H^+ desorption and is ascribed to a Coulomb explosion mechanism [31,32]. More particularly, Souda investigated He^+ ion induced H^+ desorption from H and O coadsorbed on Si and Mg surfaces, and proposed that the formation of an O 2*s* core hole in the surface OH species by quasiresonant charge exchange may initiate the subsequent desorption of H^+ ions, since the He 1*s* hole is energetically accessible to the O 2*s* electrons [21]. Metastable He atoms can also induce H^+ desorption from H_2O-Na surfaces, which is attributed to Auger decay of the incident He 1*s* hole involving one valence electron of the surface OH[22,23].

Thus, in the present cases H^+ desorption from O-H bonds of D-ribose and 2-deoxy-D-ribose films during He^+ impact may be ascribed to the formation of an O 2*s* semicore hole as a consequence of quasiresonant charge exchange. Its formation from C-H and N-H bonds in either molecule (e.g., thymine) may suggest a contribution from the Auger process, i.e., collisions of He^+ ions with C or N atom centers in the molecules ejects the two valence electrons of the C-H or N-H bond via the Auger process and thus ruptures the chemical bond, resulting in the enhanced H^+ desorption yield compared to Ar^+.

In addition to $H^{+/-}$ desorption, we also note in Fig. 4 the appearance of a discernible peak at 5 amu, which shifts to 6 amu in the case of thymine-methyl-d_3-6-*d*. These peaks clearly indicate the formation of HeH^+ and HeD^+ ions during He^+ ion irradiation of thymine and thymine-methyl-d_3-6-*d*, respectively. They are also observed during He^+ ion irradiation of 1D D-ribose films, as well as from the other molecules (Fig. 1). It may occur during the collision between backscattered He^+ ions and the relevant molecules, more particularly, the hydrogen atoms of the molecules. By decreasing the energy below 20 eV, it is also observed that He^+ ions

have a high probability to survive neutralization during collisions with the Pt substrate or the molecular films. As the QMS measures ions of 0–5 eV the appearance of He^+ ions in the 20 eV mass spectra of Fig. 4 also indicates that they can even survive multiple collision backscattering and desorb.

The HeH^+ ion is a chemically stable molecule, the formation of which via He^+ impact with H_2, or He impact with H_2^+ in the gas phase, etc., has been extensively studied both experimentally and theoretically. These collision systems provide the simplest model reactions for the study of the dynamics and mechanisms of state-to-state chemical reaction [24–27], among which He^+ collisions with H_2 may provide some clues to account for our present results. He^+ impact on H_2 can proceed via several reaction channels, such as $He^+ + H_2 \rightarrow HeH^+ + H$, or $He^+ + H_2 \rightarrow He + H^+ + H$, and others, yielding various ionic and neutral products H^+, HeH^+, H_2^+, H, He, etc. [24]. These reactions are thought to proceed via the formation of an intermediate molecular ion $(He\text{-}H_2)^{*+}$ [27]. The formation of HeH^+ ions during He^+ impact on the molecules studied here suggests the existence of a similar reaction channel, namely $He^+ + RH \rightarrow HeH^+ + R^{\cdot}$(1), probably via the formation of an intermediate molecular ion $(He\text{-}H\text{-}R)^{*+}$. Similar to He^+ ion impact on H_2, here the formation of an intermediate $(He\text{-}H\text{-}R)^+$ ion may subsequently yield another decay channel, i.e., $(He\text{-}H\text{-}R)^{*+} \rightarrow He + H^+ + R^{\cdot}$(2), which may also imply another possible contribution to the enhanced H^+ desorption observed here during He^+ impact. Another possibility is of course that either some of the HeH^+ ions are produced in excited states, which subsequently dissociate into He and H^+ during desorption from the surface, or that multiple collisions of the HeH^+ in the film prior to desorption lead to fragmentation. However, the final products are the same as in reaction channel (2).

IV. SUMMARY AND CONCLUSIONS

The interactions of hyperthermal (10–100 eV) He^+ ions with the most basic DNA (RNA) components, namely a nucleobase (thymine), the RNA and DNA sugar molecules D-ribose and 2-deoxy-D-ribose, and a nucleoside (thymidine), have been investigated using ion stimulated desorption mass spectrometry, and are compared with the Ar^+ ion impact at similar energies. Hyperthermal 10–100 eV He^+ ions induce efficient fragmentation of all investigated molecules as evidenced by the desorption of abundant ionic fragments at energies as low as 10 eV (for H^+ fragments). The chemical composition of the fragments was identified using isotope-labeled molecules. The fragment desorption spectra are similar to those obtained during Ar^+ ion irradiation, however with modulated relative intensities of the produced fragments. The underlying physical and chemical processes leading to the different observations are discussed in terms of the efficiency of momentum transfer, as well as potential energy (ionization potential) transfer, from the projectile to the target molecule (or atom), which play an important role in determining the relative intensities of the heavy and light fragments.

While H^- desorption is observed during both Ar^+ and He^+ ion irradiation of the molecules, significant desorption of H^+ is observed only during He^+ ion irradiation, and originates from either C-H, N-H, or O-H bonds. The He^+ induced H^+ desorption enhancement is likely the result of direct He^+-molecule interactions via various mechanisms, such as Auger or quasiresonant excitations of C, N, or O atom centers (or C-H, N-H, or O-H bonds) by the incident He^+ ions. Moreover, it is found that He^+ ions can abstract hydrogen atoms from the target molecules to form a HeH^+ ion; this involves either C-H, N-H, or O-H bonds, most likely via the formation of an intermediate molecular ion $(He\text{-}H\text{-}R)^{*+}$. The decay of this intermediate molecular ion, as well as collisional dissociation of desorbing HeH^+ may also contribute to the observed enhancement in H^+ desorption. Surprisingly, while He^+ is 10 times less massive than Ar^+, it is still very efficient to create smaller ring fragments from all the DNA components studied here, even at the lowest kinetic energies, which may in part be attributed to its higher ionization potential (potential energy) compared to Ar^+; this is even more so the case for H^+ production where He^+ is at least an order of magnitude more efficient than the more massive Ar^+ ion. Thus, from a radiobiological perspective, whatever He^+ lacks in mass, it makes up in internal energy, particularly for certain site specific bond damage.

ACKNOWLEDGMENTS

This work is supported by the Natural Science and Engineering Research Council of Canada and the Canadian Space Agency. A NATO collaborative linkage grant allowed staff travel to Sherbrooke (I.B.).

[1] M. Goitein, A. J. Lomax, and E. S. Pedroni, Phys. Today **55** (9), 45 (2002).
[2] D. Schulz-Ertner, A. Nikoghosyan, C. Thilmann, T. Haberer, O. Jäkel, C. Karger, G. Kraft, M. Wannenmacher, and J. Debus, Int. J. Radiat. Oncol., Biol., Phys. **58**, 631 (2004).
[3] C. von Sonntag, *The Chemical Basis for Radiation Biology* (Taylor and Francis, London, 1987).
[4] B. D. Michael and P. A. O'Neill, Science **287**, 1603 (2000).
[5] International Commission on Radiation Units and Measurements (ICRU) Report No. 31, 1979; Report No. 55, 1995.
[6] V. Cobut, Y. Frongillo, J. P. Patau, T. Goulet, M.-J. Fraser, and J.-P. Jay-Gerin, Radiat. Phys. Chem. **51**, 229 (1998).
[7] B. Boudaïffa, P. Cloutier, D. Hunting, M. A. Huels, and L. Sanche, Science **287**, 1658 (2000).
[8] M. A. Huels, B. Boudaïffa, P. Cloutier, D. Hunting, and L. Sanche, J. Am. Chem. Soc. **125**, 4467 (2003).
[9] Leon Sanche, Mass Spectrom. Rev. **21**, 349 (2002), and references therein.
[10] J. de Vries, R. Hoekstra, R. Morgenstern, and T. Schlathölter, Phys. Rev. Lett. **91**, 053401 (2003).

[11] T. Schlathölter, R. Hoekstra, and R. Morgenstern, Int. J. Mass. Spectrom. **233**, 173 (2004).
[12] W. Eberhardt, E. W. Plummer, I.-W. Lyo, R. Carr, and W. K. Ford, Phys. Rev. Lett. **58**, 207 (1987).
[13] T. LeBrun, M. Lavollée, M. Simon, and P. Morin, J. Chem. Phys. **98**, 2534 (1993).
[14] S. Ohno, H. Nagayama, K. Okazaki, and S. Sato, Bull. Chem. Soc. Jpn. **48**, 2153 (1975).
[15] Z.-W. Deng, I. Bald, E. Illenberger, and M. A. Huels, Phys. Rev. Lett. **95**, 153201 (2005).
[16] M. Imhoff, Z.-W. Deng, and M. A. Huels, Int. J. Mass. Spectrom. **245**, 68 (2005).
[17] Z.-W. Deng, M. Imhoff, and M. A. Huels, J. Chem. Phys. **123**, 144509 (2005).
[18] I. Bald, Z.-W. Deng, E. Illenberger, and M. A. Huels, Phys. Chem. Chem. Phys. **8**, 1215 (2006).
[19] Z.-W. Deng, I. Bald, E. Illenberger, and M. A. Huels Phys. Rev. Lett. **96**, 243203 (2006).
[20] F. Alvarado, S. Bari, R. Hoekstra, and T. Schlathölter, Phys. Chem. Chem. Phys. **8**, b517109a (2006).
[21] R. Souda, Int. J. Mod. Phys. B **14**, 1139 (2000).
[22] M. Kurahashi and Y. Yamauchi, Phys. Rev. Lett. **84**, 4725 (2000).
[23] T. Suzuki, M. Kurahashi, Y. Yamauchi, T. Ishikawa, and T. Noro, Phys. Rev. Lett. **86**, 3654 (2001).
[24] E. G. Jones, R. L. C. Wu, B. M. Hughes, T. O. Tiernan, and D. G. Hopper, J. Chem. Phys. **73**, 5631 (1980).
[25] D. Dhuicq, O. Lehner, F. Linder, and V. Sidis, Chem. Phys. **206**, 139 (1996).
[26] F. Aguillon, J. Chem. Phys. **109**, 560 (1998), and references therein.
[27] V. Sidis, Chem. Phys. **209**, 313 (1996).
[28] M. L. Yu and K. Mann, Phys. Rev. Lett. **57**, 1476 (1986).
[29] M. L. Yu, Nucl. Instrum. Methods Phys. Res. B **18**, 542 (1987).
[30] R. Stockbauer, D. M. Hanson, S. A. Flodström, and T. E. Madey, Phys. Rev. B **26**, 1885 (1982).
[31] S. Della-Negra, J. Depauw, H. Joret, V. Le Beyec, and E. A. Schweikert, Phys. Rev. Lett. **60**, 948 (1988).
[32] N. Kakutani, T. Azuma, Y. Yamazaki, K.-I. Komaki, and K. Kuroki, Jpn. J. Appl. Phys., Part 2 **34**, L580 (1995).